Journal of Basics and Applied Sciences Research (JOBASR)
ISSN (print): 3026-9091, ISSN (online): 1597-9962
Volume 3(3) May 2025
DOI: https://dx.doi.org/10.4314/jobasr.v3i3.28

The influence of J_6 zonal harmonics on the location and stability of the CEPs of a Nigerian satellite in the generalized R3BP for EQ Pegasi system

Gyegwe, J. M.[1*], Omede, S.[2], Ibrahim, M. A.[3] and Momoh, S. O.[4]
[1,2,3 & 4]Department of Mathematics, Faculty of Science, Federal University Lokoja, Kogi State, Nigeria.
Corresponding Author Email: [1]jessica.gyegwe@fulokoja.edu.ng
[2]solomonomede1@gmail.com; [3]sheidu.momoh@fulokoja.edu.ng; [4]musa.ibrahim@fulokoja.edu.ng

ABSTRACT
In this study, the generalized restricted three-body problem (R3BP) is applied to the EQ Pegasi binary system to investigate the effects of zonal harmonics on the motion of a satellite. Building on previous research, it enhances the standard potential function to represent the oblateness of the primaries by adding higher-order zonal harmonic terms J_2, J_4 and J_6 for both the primary and secondary bodies. After establishing the equations regulating motion, the collinear equilibrium points (CEPs) are found numerically using the Newton-Raphson technique. The Lyapunov stability theorem is used to assess their stability. According to the results, the addition of zonal harmonics somewhat changes the locations of the CEPs, with the equatorial bulge J_2 having the most significant impact. The Jacobian constants indicate the energy levels at these moments, showing slightvariations across different scenarios. Even after adding higher-order zonal harmonics, stability evaluations show that the CEPs are still unstable, which aligns with classical R3BP findings. The necessity of active station-keeping in satellite mission planning, particularly close to these locations, is highlighted by this ongoing volatility. The study highlights the importance of considering higher-order gravitational effects while designing missions and analyzing stability, particularly for Nigerian spacecraft operating in complicated gravitational fields. The findings underscore the importance of advanced modeling in addressing the complex dynamics of binary star systems, thereby supporting earlier studies and offering valuable insights for future space missions.

Keywords:
Zonal harmonics,
Nigerian satellite,
Collinear Equilibrium Points,
Stability,
EQ Pegasi,
Newton-Raphson technique.

INTRODUCTION

The field of celestial mechanics has been crucial for comprehending the movements of artificial satellites, space probes, and natural celestial entities. The restricted three-body problem (R3BP) is a central challenge in this domain, providing a simplified yet effective framework for examining the gravitational interactions that affect a small mass due to the presence of two larger bodies. In the classical restricted three-body problem, five Lagrange points (equilibrium points; L_1, L_2, L_3, L_4, and L_5) exist in the rotating frame where primaries are fixed. The equilibrium points L_1, L_2, and L_3 are collinear and unstable due to saddle-point dynamics, while L_4 and L_5, forming triangular configurations with the primary, are stable if $\mu = \frac{m_2}{m_1 + m_2} < 0.0385$ (Szebehely(1967). Various aspects of the R3BP, such as equilibrium points and their stability, periodic and quasi-periodic orbits, resonance phenomena, chaotic behavior, and perturbative effects from additional forces like PR-Drag, Stoke's Drag, Albedo, radiation pressure, oblateness,angular velocity variation, variable mass, Triaxillity and relativistic corrections have been extensively studied by researchers (see Singh *et al.*, (2016, 2017, 2018); Kalantonis *et al.*, 2021; Kalantonis 2025; Gyegwe *et al.*, 2022; Baresi and Dell'Elce 2023; Jain and Aggarwal, 2015; Pan and Hou, 2022; Oni *et al.*, 2024; Singh and Ashagwu 2024; Singh and Tyokaa, 2022; Putra *et al.*, 2024; Arredondo *et al.*, 2012; Katour *et al.*, 2014; Roy, 2005). These studies highlight those deviations from idealized scenarios, such as assuming spherical primary bodies, significantly increase the complexity of the system's dynamics.

How to cite this article: Gyegwe, J. M., Omede, S., Ibrahim, M. A. and Momoh, S. O. (2025). The influence of J_6 zonal harmonics on the location and stability of the CEPs of a Nigerian satellite in the generalized R3BP for EQ Pegasi system. *Journal of Basics and Applied Sciences Research, 3*(3), 261-276. https://dx.doi.org/10.4314/jobasr.v3i3.28

Zonal harmonics describe the deviation of a celestial body's gravitational potential from a perfect sphere, influencing the motion of satellites in orbit. The external gravitational potential of an oblate body, expressed in terms of Legendre polynomials, has been extensively analyzed Lambeck (1988); Murray & Dermott (1999); Abouelmadg *et al.*, (2015b). These studies are highly applicable to mission design, station-keeping strategies, and trajectory optimization in the context of space exploration.

To further Nigeria's space exploration objectives, the Federal Ministry of Innovation, Science, and Technology established the National Space Research and Development Agency (NASRDA) in Abuja on May 5, 1999. Despite financial and infrastructure obstacles, NASRDA, which former President Olusegun Obasanjo founded, has launched five satellites. These include NigComSat-1 (2007, lost in 2008) for communications, NigeriaSat-2 and NigeriaSat-X (2011) for advanced imaging, NigeriaSat-1 (2003) for disaster and resource monitoring, and NigComSat-1R (2011) as a successor (Oyewole, 2017). Through its UN-SPIDER office, NASRDA promotes disaster management, oversees specialist centers, and collaborates with the UK, China, and Russia. Nigeria's leadership in African space technology is expected to be strengthened by future initiatives, such as Edusat-2 and a lunar probe, by 2030, which will leverage the country's equatorial location to enhance launch capabilities (Oyewole, 2024).

The Pegasus constellation contains the cataclysmic variable binary system PQ Pegasi, which comprises a white dwarf and a red dwarf. In contrast to the white dwarf, which is a compact, dense remnant of a star that is smaller but more massive due to its high density, the red dwarf is a bigger star that is still in its main sequence stage. As the material is drawn from the red dwarf by the white dwarf, the system exhibits dramatic activity, resulting in sporadic brightness surges. The red dwarf is called the "donor star," and the white dwarf is the "accretor." None of the stars are given individual names; instead, they are referred to by their roles (Crosley and Osten, 2018). A summary of related works is presented in Table 1.

This study considers an artificial satellite (any of the five Nigerian satellites released into orbit) as an infinitesimal mass moving under the gravitational field of a binary system, taking EQ Pegasi as a representative system. The oblateness parameters of the primary and secondary bodies are introduced to refine the classical potential function. Building upon previous studies (Abouelmagd, 2012; Abouelmagd *et al.*, 2015a), the research derives motion equations that incorporate zonal harmonics' effects. It employs numerical techniques, such as the Newton-Raphson method, to determine collinear equilibrium points (CEPs), and applies the Lyapunov stability theorem to analyze the locations of the CEPs. The novelty of this work lies in the explicit consideration of J_6 zonal harmonic terms in the EQ Pegasi system.The contributions of this study include:

- Enhanced Gravitational Modeling in the R3BP: The study extends the classical Restricted Three-Body Problem (R3BP) by incorporating higher-order zonal harmonics (J_2, J_4, J_6) for both celestial bodies in the EQ Pegasi binary system. This refinement moves beyond the simple spherical approximation, offering a more precise representation of gravitational forces.
- Implications for Nigerian Space Missions: The research investigates the orbital dynamics of Nigeria's satellites (e.g., NigComSat-1R, NigeriaSat-2, etc.) within the complex gravitational field of a binary star system. These findings support mission planning and satellite operations for Nigeria's space initiatives.
- Precision Localization of Collinear Equilibrium Points (CEPs): The study accurately determines the positions of CEPs under perturbed conditions using the Newton-Raphson iterative method.
- Stability Analysis Using Lyapunov's Criterion: The study confirms the inherent instability of CEPs, even when higher-order harmonics are considered, aligning with classical R3BP predictions. This underscores the need for continuous orbital corrections in mission design.
- Comprehensive Parametric Investigation: Nine distinct cases involving oblateness parameters are analyzed, generating detailed results on CEP positions and Jacobian constants (Tables 3–5). These are further illustrated through graphical depictions (e.g., Figure 4) for enhanced clarity.

Practical Insights for Space Exploration: The research highlights higher-order gravitational perturbations' subtle yet significant influence, underscoring their critical role in trajectory optimization and stability assessments for missions in binary star systems.

The paper is organized as follows: Section 2 provides the mathematical formulation of the model, the computation and the stability analysis of the CEPs. Sections 3 results and discuss, and sections 4 conclude the study's results.

Table 1: A summary of related works

Author(s) & Year	Focus of Study	Key Contribution	System Studied	Methodology
Szebehely (1967)	Classical R3BP	Established the foundational theory of orbits and equilibrium points in R3BP	General	Analytical
Lambeck (1988)	Zonal harmonics in gravitational potential	Analyzed Earth's gravitational field deviations using Legendre polynomials	Earth	Analytical
Abouelmagd (2012)	R3BP with oblateness	Studied triangular points' stability with J_2 effects	General	Analytical/Numerical
Abouelmagd *et al.*, (2015a)	R3BP with zonal harmonics (J_2, J_4)	Extended R3BP to include J_2 and J_4 for both primaries, assessed stability	General	Analytical/Numerical
Singh *et al.*, (2016)	R3BP with triaxial and oblate primaries	Investigated periodic motions around CEPs with additional perturbations	General	Numerical
Bury & McMahon (2020)	Zonal harmonics near secondary body	Examined dynamical structures influenced by zonal harmonics in CR3BP	General	Numerical
Singh & Ashagwu (2024)	Elliptic R3BP with PR-drag and oblateness	Analyzed triangular points' stability with combined effects	General	Analytical/Numerical
Oni *et al.*, (2024)	R3BP with variable shape and masses	Investigated out-of-plane dynamics with evolving primaries (from document, authoritative)	General	Numerical
Kalantonis, (2025)	The influence of oblateness on asymptotic orbits in the Hill three-body problem	Analysis and characterization of homoclinic and heteroclinic connections associated with CEPs, determining conditions for the	Modified Hill three-body problem with an oblate primary body	Combination of analytical and numerical methods, including systematic variation of the oblateness parameter, computation of stable and unstable

		existence and location of these orbits under varying oblateness parameters		invariant manifolds, and use of differential correction techniques leveraging system symmetries

MATERIALS AND METHODS

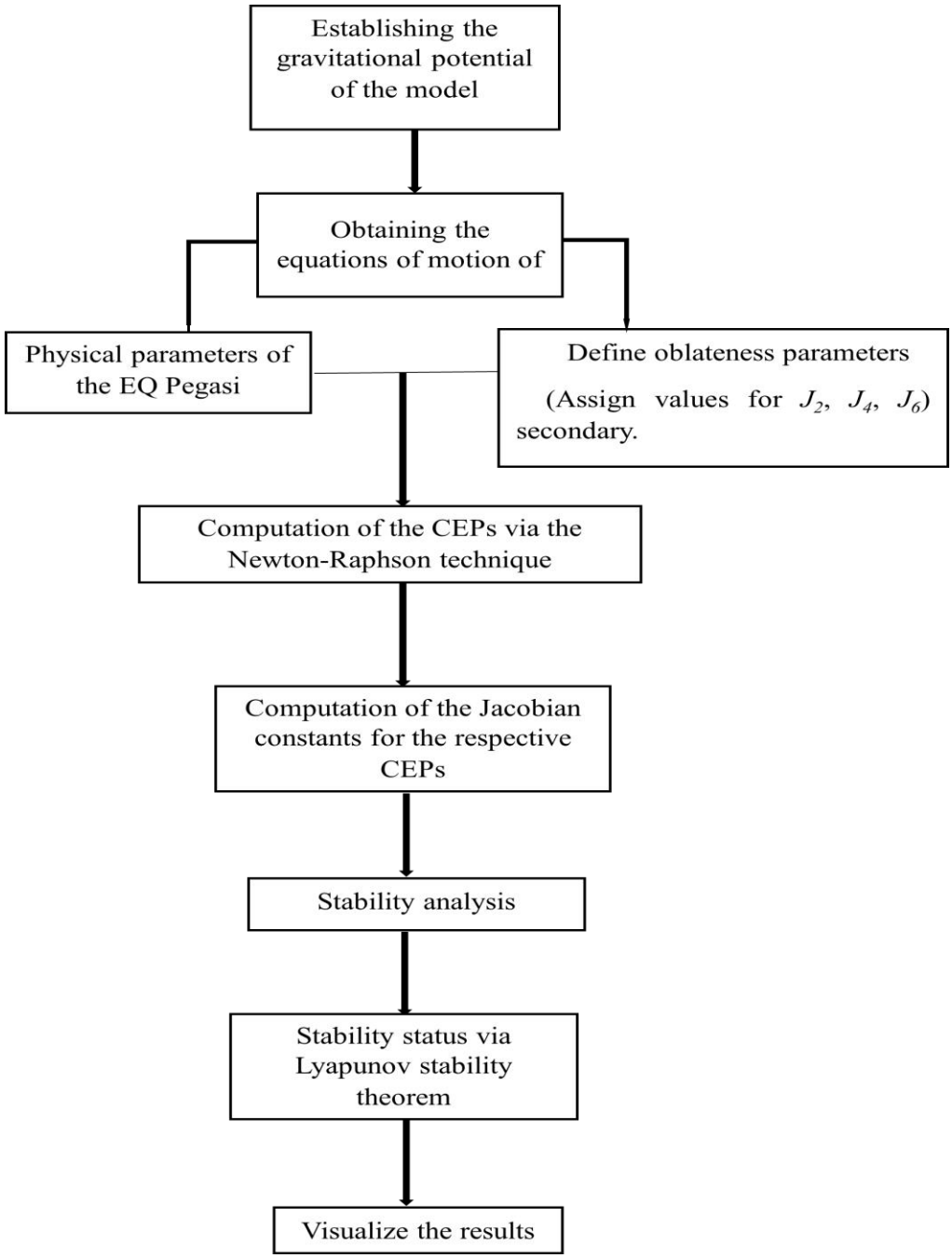

Figure 1: Flowchart for Procedures/Simulation Methods

Mathematical formulation of the Problem

Zonal harmonics of the oblate spheroidal primaries

The external gravitational potential of an oblate body can be expressed in terms of Legendre polynomials as:

$$V = \frac{-GM_\lambda}{r}\left[1-\sum_{n=2}^{+\infty} J_n\left(\frac{R_\lambda}{r}\right)P_n Sin(\theta)\right], \quad (1)$$

where,

the parameter G denotes the gravitational constant, M_λ is the mass of the body, r is the distance from the centre of the body to any other body, θ is the polar angle from the axis of rotation, R_λ is the equatorial radius of the body, J_n is the dimensionless coefficient that characterizes the size of the non-spherical components of the potential and $P_n Sin(\theta)$ represent the Legendre Polynomials of degree n. According to Abouelmagd (2012), $\theta = 0$ under the assumption that the primary body's equatorial plane of motion coincides with the system's plane of motion. In terms of $P_n Sin(\theta)$, we can also have

$$P_n(x) = \frac{1}{2^n n!}\frac{d^n}{dx^n}(x^2-1). \quad (2)$$

The evaluation of Eqn. (2) for the aforementioned conditions shows that for odd values of n, $P_n(0) = 0$, and consequently, the external gravitational potential of the oblate body for $n = 2,...,6$ is obtained as (see also Abouelmagd (2012); Abouelmagd et al.(2015a,b)):

$$V = -GM_\lambda\left[\frac{1}{r}+\frac{J_2R_\lambda^2}{2r^3}-\frac{3J_4R_\lambda^4}{8r^5}+\frac{5J_6R_\lambda^6}{16r^7}\right] \quad (3)$$

Taking into consideration two oblate spheroids and assuming that their masses are M_1 and M_2 such that $M_1 > M_2$, then the external gravitational potential between the two masses can be obtained as:

$$V = \frac{-GM_1M_2}{r}\left[\begin{array}{l}1+\left(\frac{A_1^*}{2r^2}-\frac{3A_2^*}{8r^4}+\frac{5A_3^*}{16r^6}\right)\\ +\left(\frac{A_1^{**}}{2r^2}-\frac{3A_2^{**}}{8r^4}+\frac{5A_3^{**}}{16r^6}\right)\end{array}\right], \quad (4)$$

where

$A_i^* = J_{2i}R_{\lambda_1}^{2i}$ and $A_i^{**} = J_{2i}^*R_{\lambda_2}^{2i}$ as well as J_{2i} and $J_{2i}^*, (i = 1,2,3)$ are the oblateness and zonal harmonics coefficients of the primary and secondary bodies, respectively.

Equations of motion

In this section, the equations of motion of the satellite is presentedwhile taking into cognizance the oblateness coefficients A_1^*, A_2^*, A_3^* and A_1^{**}, A_2^{**}, A_3^{**} corresponding to the primary and secondary bodies, respectively, of the restricted three-body problem. Following the procedures presented in Szebehely (1967), Roy (2005), and Bury and McMahon (2020); consider three bodies with masses M_1, M_2 and M_0. The parameters M_1 and M_2 are significant, and the corresponding bodies are called primaries, while the mass M_0 of the third body is negligible. In this investigation, the third body, also known as the infinitesimal mass, is taken as a satellite orbiting or rotating under the gravitational attraction of the EQ Pegasi system.

The normalization of the R3BP in carried out by choosing to make $M_1 + M_2 = 1$ (the sum of the masses equal to unity), $M_1 = 1-\mu$, $M_2 = \mu \le \frac{1}{2}$, gravitational constant $G = 1$ and the distance between the primaries is assumed to be unity. In the inertial reference frame, the coordinates of the bodies with masses M_1, M_2 and M_0 are given as (ξ_1, η_1, ζ_1), (ξ_2, η_2, ζ_2) and (ξ, η, ζ), respectively, while in the rotating reference frame, the coordinates of M_1, M_2 and M_0 are $(\mu, 0, 0)$, $(\mu-1, 0, 0)$ and (x, y, z), correspondingly. The mean motion (angular velocity) of the primaries denoted by n is assumed to be equal to one about the z-axis which coincides with the ζ-axis. These descriptions and assumptions are shown in Figure 2.

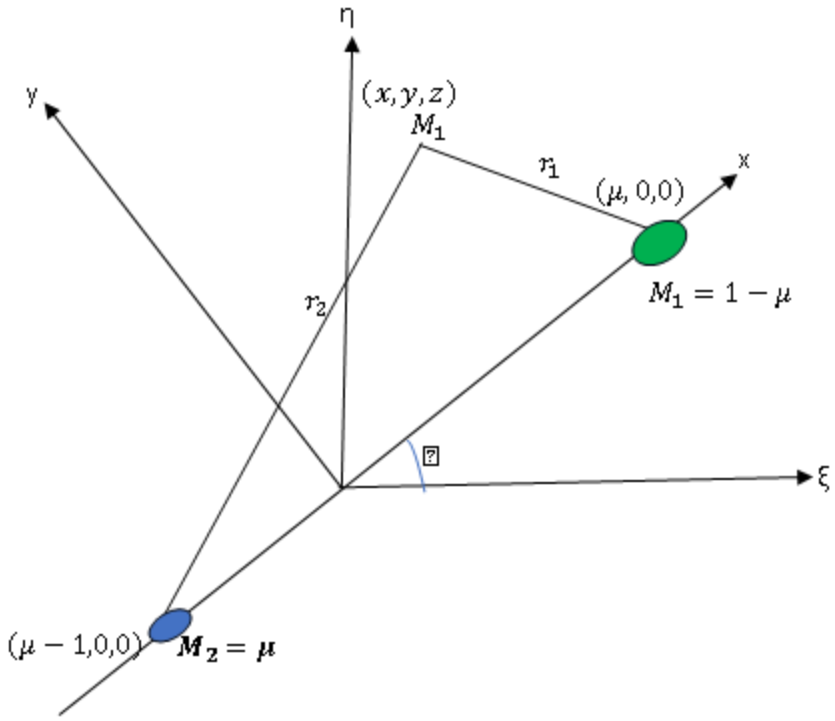

Figure 2: The inertial (ξ,η,ζ) and synodic (x,y,z) reference frames for the RTBP with oblate primaries

The equations of motion of the artificial satellite have been obtained as:

$$\begin{aligned}\ddot{x}-2n\dot{y}&=\Omega_x,\\ \ddot{y}-2n\dot{x}&=\Omega_y,\\ \ddot{z}&=\Omega_z,\end{aligned} \tag{5}$$

where

$$\Omega=\frac{n^2}{2}(x^2+y^2)+(1-\mu)\left[\frac{1}{r_1}+\frac{A_1^*}{2r_1^3}-\frac{3A_2^*}{8r_1^5}+\frac{5A_3^*}{16r_1^7}\right]+\mu\left[\frac{1}{r_2}+\frac{A_1^{**}}{2r_2^3}-\frac{3A_2^{**}}{8r_2^5}+\frac{5A_3^{**}}{16r_2^7}\right]$$
$$-(1-\mu)\left[\frac{3A_1^*}{2r_1^5}-\frac{15A_2^*}{8r_1^7}+\frac{35A_3^*}{16r_1^9}\right]z^2-\mu\left[\frac{3A_1^{**}}{2r_2^5}-\frac{15A_2^{**}}{8r_2^7}+\frac{35A_3^{**}}{16r_2^9}\right]z^2, \tag{6}$$

is the potential function, also known as the force function, while the distance between the primary and the satellite as well as the distance between the secondary and the satellite are

$$r_1=\sqrt{(x-\mu)^2+y^2+z^2}\ \text{ and }\ r_2=\sqrt{(x-\mu+1)^2+y^2+z^2} \tag{7}$$

respectively. The mean motion of the satellite is denoted by

$$n^2=1+\frac{3}{2}\left(A_1^*+A_1^{**}\right)-\frac{15}{8}\left(A_2^*+A_2^{**}\right)+\frac{35}{16}\left(A_3^*+A_3^{**}\right) \tag{8}$$

Partially differentiating Eqns. (2) w.r.t. x, y and z correspondingly, we get

$$\Omega_x = \mathrm{n}^2 x-(1-\mu)\left(\frac{x-\mu}{r_1^3}+\frac{3A_1^*(x-\mu)}{2r_1^5}\left(1-\frac{5z^2}{r_1^2}\right)-\frac{15A_2^*(x-\mu)}{8r_1^7}\left(1-\frac{7z^2}{r_1^2}\right)+\frac{35A_3^*(x-\mu)}{16r_1^9}\left(1-\frac{9z^2}{r_1^2}\right)\right)-\mu\left(\frac{x-\mu+1}{r_2^3}+\frac{3A_1^{**}(x-\mu+1)}{2r_2^5}\left(1-\frac{5z^2}{r_2^2}\right)-\frac{15A_2^{**}(x-\mu+1)}{8r_2^7}\left(1-\frac{7z^2}{r_2^2}\right)+\frac{35A_3^{**}(x-\mu+1)}{16r_2^9}\left(1-\frac{9z^2}{r_2^2}\right)\right), \tag{9a}$$

$$\Omega_y = n^2 y+(1-\mu)z^2 y\left(\frac{15A_1^*}{2r_1^7}-\frac{105A_2^*}{8r_1^9}+\frac{315A_3^*}{16r_1^{11}}\right)-(1-\mu)y\left(\frac{1}{r_1^3}+\frac{3A_1^*}{2r_1^5}-\frac{15A_2^*}{8r_1^7}+\frac{35A_3^*}{16r_1^9}\right)+\mu z^2 y\left(\frac{15A_1^{**}}{2r_2^7}-\frac{105A_2^{**}}{8r_2^9}+\frac{315A_3^{**}}{16r_2^{11}}\right)-\mu y\left(\frac{1}{r_2^3}+\frac{3A_1^{**}}{2r_2^5}-\frac{15A_2^{**}}{8r_2^7}+\frac{35A_3^{**}}{16r_2^9}\right), \tag{9b}$$

and

$$\Omega_z = -2(1-\mu)z\left(\frac{1}{2r_1^3}+\frac{9A_1^*}{4r_1^5}-\frac{45A_2^*}{8r_1^7}+\frac{105A_3^*}{32r_1^9}\right)+(1-\mu)z^3\left(\frac{15A_1^*}{2r_1^7}-\frac{105A_2^*}{8r_1^9}+\frac{315A_3^*}{16r_1^{11}}\right)-2\mu z\left(\frac{1}{2r_2^3}+\frac{9A_1^{**}}{4r_2^5}-\frac{45A_2^{**}}{8r_2^7}+\frac{105A_3^{**}}{32r_2^9}\right)+\mu z^3\left(\frac{15A_1^{**}}{2r_2^7}-\frac{105A_2^{**}}{8r_2^9}+\frac{315A_3^{**}}{16r_2^{11}}\right). \tag{9c}$$

Constant of Integration

Multiplying Eqns. (5) by $\dot{x}, \dot{y}$ and $\dot{z}$ respectively, and adding, we get

$$\dot{x}\ddot{x}+\dot{y}\ddot{y}+\dot{z}\ddot{z} = \Omega_x\dot{x}+\Omega_y\dot{y}+\Omega_z\dot{z}.$$

The constant of integration, otherwise known as the Jacobian constant, C, is obtained after integrating the last equation as:

$$\dot{x}^2+\dot{y}^2+\dot{z}^2 = 2\Omega-C \tag{10}$$

Equation (10) can also be written as

$$v^2 = 2\Omega-C \tag{11}$$

where v is the magnitude of the satellite's velocity in the synodic reference frame.

By substituting Eqn. (6) into (11), the Jacobian constant is obtained as

$$C = -\dot{x}^2-\dot{y}^2-\dot{z}^2+n^2(x^2+y^2)+2(1-\mu)\left[\frac{1}{r_1}+\frac{A_1^*}{2r_1^3}-\frac{3A_2^*}{8r_1^5}+\frac{5A_3^*}{16r_1^7}\right]+2\mu\left[\frac{1}{r_2}+\frac{A_1^{**}}{2r_2^3}-\frac{3A_2^{**}}{8r_2^5}+\frac{5A_3^{**}}{16r_2^7}\right]-2(1-\mu)\left[\frac{3A_1^*}{2r_1^5}-\frac{15A_2^*}{8r_1^7}+\frac{35A_3^*}{16r_1^9}\right]z^2-2\mu\left[\frac{3A_1^{**}}{2r_2^5}-\frac{15A_2^{**}}{8r_2^7}+\frac{35A_3^{**}}{16r_2^9}\right]z^2 \tag{12}$$

Location of Collinear equilibrium points

The equilibrium points are locations where the gravitational forces and the centrifugal force due to the rotating reference frame balance each other out, resulting in zero net force on the infinitesimal body. That is, when the velocity and acceleration due to the satellite equals zero. The CEPs are determined by $\Omega_x = \Omega_y = \Omega_z = 0$, when $y = z = 0$.

From Eqns. (9a), we have

$$\Omega_x(x,0,0) = \mathrm{n}^2 x - (1-\mu)\left(\frac{x-\mu}{|x-\mu|^3} + \frac{3A_1^*(x-\mu)}{2|x-\mu|^5} - \frac{15A_2^*(x-\mu)}{8|x-\mu|^7} + \frac{35A_3^*(x-\mu)}{16|x-\mu|^9}\right)$$
$$-\mu\left(\frac{x-\mu+1}{|x-\mu+1|^3} + \frac{3A_1^{**}(x-\mu+1)}{2|x-\mu+1|^5} - \frac{15A_2^{**}(x-\mu+1)}{8|x-\mu+1|^7} + \frac{35A_3^{**}(x-\mu+1)}{16|x-\mu+1|^9}\right) = 0. \quad (13)$$

The CEPs are the solutions of Eqn. (13). The Newton-Raphson Technique is employed to find the roots of the equation.

Table 2: The physical details of EQ Pegasi

Binary System	Mass of Primary (M_1)	Mass of Secondary (M_2)	Mass parameter (μ)
EQ Pegasi	0.33 M_S	0.16 M_S	0.32653

In Table 2, the physical characteristics of EQ Pegasi, as retrieved from Johnson (2022), are presented. The first, second, and third columns furnish the mass of the primary M_1, the mass of the secondary M_2 (as compared with the mass of the Sun)and the mass ratio of the binary system, μ, respectively.

Table 3: The values of the oblateness parameters of EQ Pegasi for nine distinct cases up to J_6 Zonal Harmonics

Case	A_1^*	A_1^{**}	A_2^*	A_2^{**}	A_3^*	A_3^{**}
1.	0.004	0.001	–0.0012	–0.0002	0.00004	0.00002
2.	0.005	0.002	–0.0013	–0.0003	0.00005	0.00003
3.	0.006	0.003	–0.0014	–0.0004	0.00006	0.00004
4.	0.007	0.004	–0.0015	–0.0005	0.00007	0.00005
5.	0.008	0.005	–0.0016	–0.0006	0.00008	0.00006
6.	0.009	0.006	–0.0017	–0.0007	0.00009	0.00007
7.	0.010	0.007	–0.0018	–0.0008	0.00010	0.00008
8.	0.011	0.008	–0.0019	–0.0009	0.00011	0.00009
9.	0.012	0.009	–0.0020	–0.0010	0.00012	0.00010

In Table 3, the values of the oblateness parameters of EQ Pegasi for nine distinct cases for J_2(A_1^*, A_1^{**}), J_4(A_2^*, A_2^{**}) and J_6(A_3^*, A_3^{**}) Zonal Harmonics are presented. The values of the oblateness parameters have been assumed, similar to those used in Abouelmagd et al. (2015a). The second and third columns present the J_2 values for the primary and secondary. Similarly, the J_4 and J_6 values are presented in the fourth fifth, and sixth and seventh columns respectively. It can be observed that the J_4 values are negative differing from the J_2, and J_6 positive values. The gravitational potential of Earth is characterized by a negative J_4 the term, which contrasts with the dynamics of binary star systems such as PQ Pegasi. On Earth, zonal harmonics describe deviations from a perfect spherical gravitational potential, with J_2 reflecting the equatorial bulge caused by Earth's rotation (Lambeck, 1988) and J_4 representing higher-order deformations. The negative sign of J_4 is attributed to the mass distribution at higher latitudes, Earth's rotation, and the chosen sign convention for expansion coefficients (Reigber, 1989). In contrast, binary star systems exhibit complex dynamics, with gravitational potentials influenced by mass distribution, symmetry, orbital motion, tidal forces, and rotational distortions (Murray & Dermott, 1999). The sign and relevance of higher-order terms in binary systems depend on detailed modeling, which may reveal positive or negative J_4-like terms resulting from tidal elongation or flattening effects (Fabian *et al.*, 2012). However, for the purpose of this research work, the J_4 parameters for EQ Pegasi have been assumed to be negative.

Table 4: The CEPs and corresponding Jacobian constants of the satellites with respect to (w.r.t.) PQ Pegasi for J_6 Zonal Harmonics for the nine cases in Table 3

Case	$L_1(x,0)$	$L_2(x,0)$	$L_3(x,0)$	C_{L_1}	C_{L_2}	C_{L_3}
1.	−0.2485171	1.1339766	−1.2498033	3.9597402	3.3301836	3.5637225
2.	−0.2481378	1.1337147	−1.2499801	3.9677197	3.3353756	3.5702860
3.	−0.2477673	1.1334551	−1.2501546	3.9756943	3.3405672	3.5768492
4.	−0.2474054	1.1331977	−1.2503267	3.9836643	3.3457582	3.5834121
5.	−0.2470517	1.1329425	−1.2504965	3.9916298	3.3509488	3.5899748
6.	−0.2467060	1.1326895	−1.2506641	3.9995909	3.3561389	3.5965371
7.	−0.2463680	1.1324387	−1.2508296	4.0075479	3.3613286	3.6030992
8.	−0.2460373	1.1321900	−1.2509929	4.0155007	3.3665176	3.6096610
9.	−0.2457139	1.1319433	−1.2511541	4.0234497	3.3717062	3.6162226

Table 5: The Collinear Equilibrium Points and corresponding Jacobian constants of PQ Pegasi for J_4 Zonal Harmonics using the nine cases in Table 3

Case	$L_1(x,0)$	$L_2(x,0)$	$L_3(x,0)$	C_{L_1}	C_{L_2}	C_{L_3}
1.	−0.2496702	1.1346394	−1.2498363	3.9730523	3.3353260	3.5686553
2.	−0.2488998	1.1343856	−1.2502588	3.9836489	3.3411499	3.5761941
3.	−0.2481613	1.1341343	−1.2506731	3.9942247	3.3469735	3.5837311
4.	−0.2474527	1.1338858	−1.2510795	4.0047813	3.3527965	3.5912665
5.	−0.2467719	1.1336398	−1.2514783	4.0153196	3.3586191	3.5988002
6.	−0.2461173	1.1333964	−1.2518697	4.0258407	3.3644412	3.6063324
7.	−0.2454871	1.1331554	−1.2522537	4.0363457	3.3702628	3.6138631
8.	−0.2448801	1.1329170	−1.2526307	4.0468354	3.3760840	3.6213923
9.	−0.2442947	1.1326810	−1.2530011	4.0573106	3.3819048	3.6289201

Table 6: The Collinear Equilibrium Points and corresponding Jacobian constants of PQ Pegasi for J_2 Zonal Harmonics using the nine cases in Table 3

Case	$L_1(x,0)$	$L_2(x,0)$	$L_3(x,0)$	C_{L_1}	C_{L_2}	C_{L_3}
1.	−0.2470833	1.1339893	−1.2505497	3.9666881	3.3313783	3.5658325
2.	−0.2459000	1.1336868	−1.2511135	3.9774632	3.3369266	3.5732634
3.	−0.2447765	1.1333872	−1.2516650	3.9881903	3.3424743	3.5806913
4.	−0.2437077	1.1330904	−1.2522047	3.9988729	3.3480212	3.5881162
5.	−0.2426889	1.1327963	−1.2527331	4.0095142	3.3535675	3.5955383
6.	−0.2417162	1.1325051	−1.2532504	4.0201172	3.3591132	3.6029577
7.	−0.2407861	1.1322165	−1.2537572	4.0306843	3.3646582	3.6103744
8.	−0.2398954	1.1319307	−1.2542538	4.0412179	3.3702026	3.6177885
9.	−0.2390414	1.1316474	−1.2547405	4.0517201	3.3757463	3.6252002

The CEPs and corresponding Jacobian constants of the satellite with respect to (w.r.t.) EQ Pegasi up to J_6 Zonal Harmonics for the nine cases in Table 3 are provided in Table 4. The second, third, and fourth columns present the first, second, and third CEPs $L_{1,2,3}$. It can be observed that a move from cases 1 through 9 shows a slight increase for L_1 and a slight decrease for L_2 both points shifting towards the origin while L_3 decreases and shifts away from the origin. Figure 3 is a graphical representation of the CEPs in the EQ Pegasi system. It's a two-dimensional plot for the $xy-coordinate$ system showing the bigger primary M_1 placed closer to the origin while M_2 lies further out on the right on the $x-axis$. Also, the equilibrium point L_1 lies

between the primaries M_1 and M_2, while L_2 is to the right of M_2 and L_3 to the left of M_1 on the $x-axis$ .The fifth, sixth, and seventh columns give the values of the Jacobian constant $C_{L_{1,2,3}}$ at $L_{1,2,3}$, respectively. Similarly, the CEPs and corresponding Jacobian constants of the satellite w.r.t. EQ Pegasi for the zonal harmonics J_4 as well as J_2 are given in Tables 5 and 6, respectively. The values show similar patterns to those in Table 4.

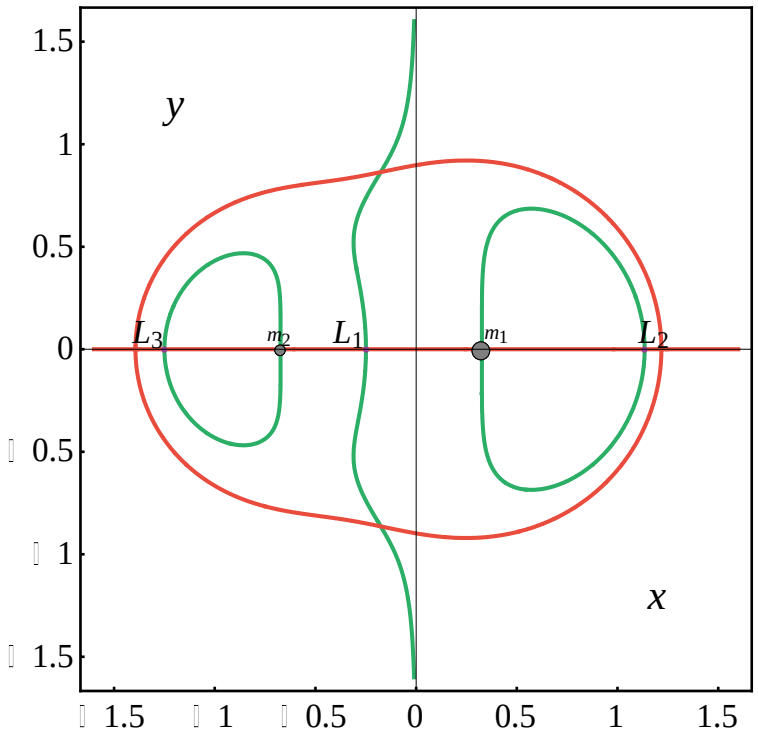

Figure 3: The positions of the CEPs $L_{1,2,3}$ and the masses m_1 and m_2 of the primary and secondary stars respectively for the first case in Table 3

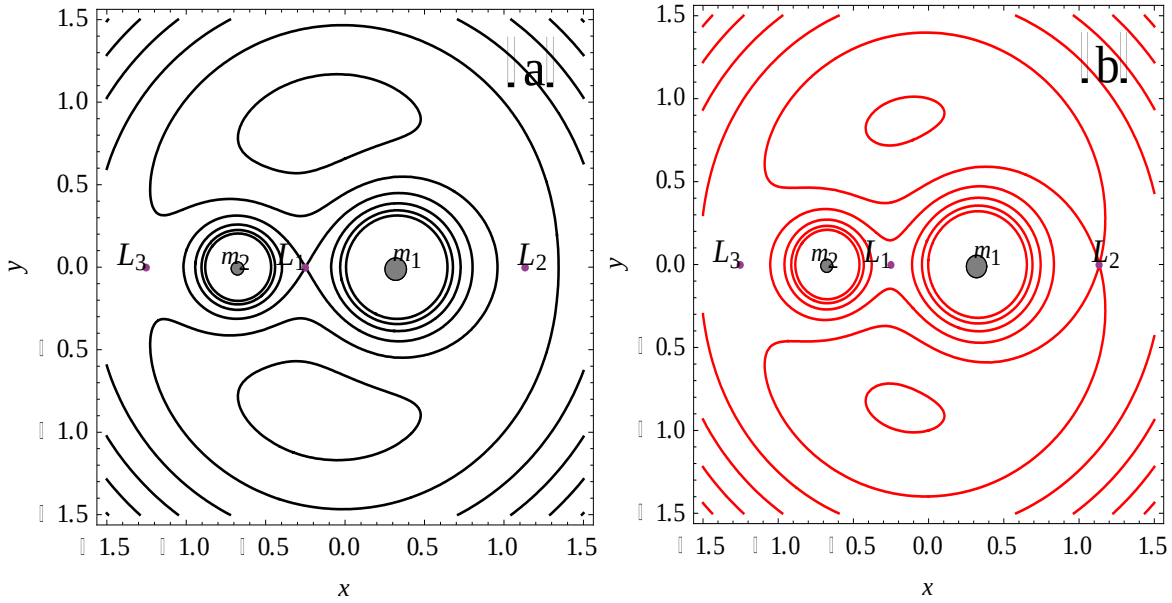

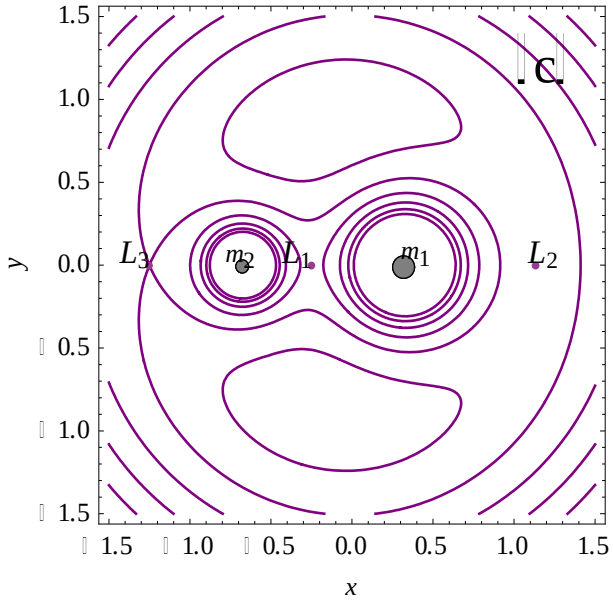

Figure 4: The zero velocity curves corresponding to Case 1 of Table 3

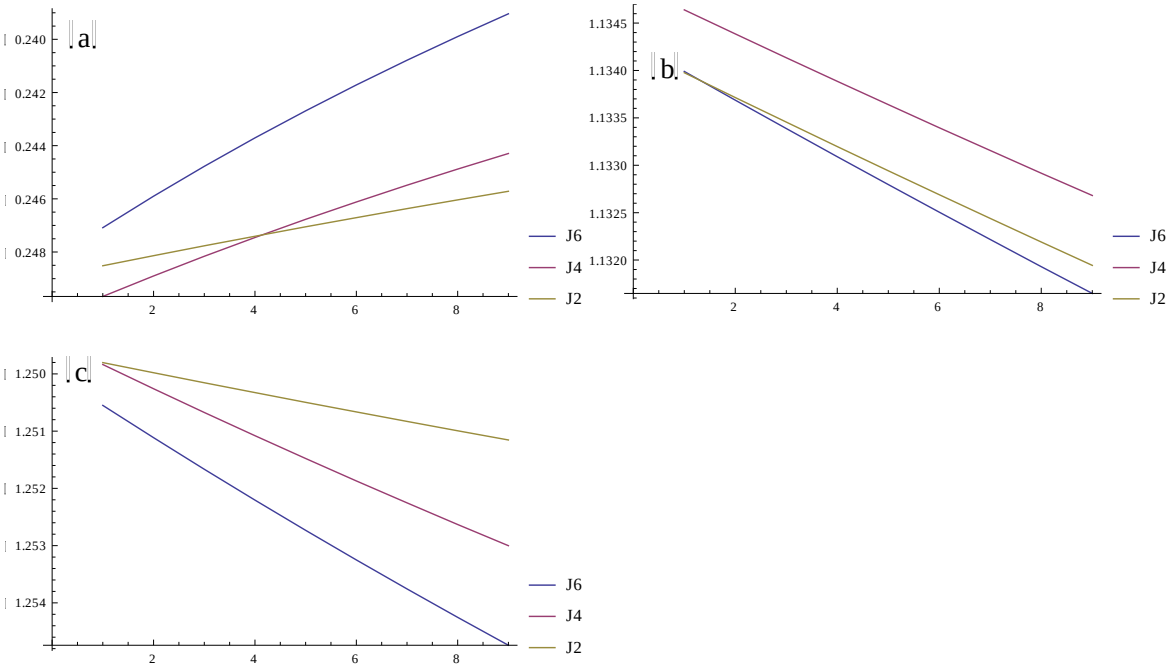

Figure 5 (a), (b), (c): The Collinear Equilibrium Points $L_{1,2,3}$ corresponding to (a), (b), and (c) showing the Zonal harmonics J_2, J_4, J_6 in gray, magenta, and blue lines respectively

The impacts of the zonal harmonics J_2, J_4, and J_6 on the locations of the collinear equilibrium points (CEPs) are depicted in Figure 4. Their contributions are differentiated by a color-coded scheme: gray for J_2, magenta for J_4, and blue for J_6. The data in Tables 4, 5, and 6, which provide details on the CEPs and their associated Jacobian constants for nine cases of oblateness parameters listed in Table 3, were used to derive the figure. In Figure 5, each panel represents a distinct equilibrium point: panel (a) for L_1, panel (b) for L_2, and panel (c) for L_3. The color scheme illustrates the impact of each harmonic on the CEPs, with J_2 denoting the equatorial bulge, J_4 representing higher-

order deformations and J_6 Indicating finer gravitational asymmetries. By including J_4 and J_6, the gravitational potential it is refined beyond the primary influence of J_2, resulting in additional perturbations that alter the CEPs. These shifts are illustrated visually, showing how higher-order terms progressively alter the equilibrium positions.

Stability of Collinear Points

The Variational Equation

To study the motion near any of the equilibrium points $L(x_0, y_0)$, we write

$x = x_0 + \xi$, and $y = y_0 + \eta$,

where ξ and η are small displacements in (x_0, y_0).

For the collinear points $L_{1,2,3}$, we have $x_0 = x_{1,2,3}$, $y_0 = 0$.

By making

$$\dot{x} = \dot{\xi}, \quad and \quad \dot{y} = \dot{\eta},$$
$$\ddot{x} = \ddot{\xi}, \qquad \ddot{y} = \ddot{\eta},$$

as well as expanding Eqn. (6) by means of Taylor series expansion while considering only the 2-D problem, we have

$$\ddot{\xi} - 2n\dot{\eta} = \Omega^0_{xx}\xi + \Omega^0_{xy}\eta,$$
$$\ddot{\eta} - 2n\dot{\xi} = \Omega^0_{xy}\xi + \Omega^0_{yy}\eta. \qquad (14)$$

Eqn. (14) is called the variational equation with respect to Eqns. (5). Here, only linear terms in ξ and η have been taken. The second partial derivatives of Ω are denoted by subscripts. The superscript 0 indicates that the derivatives are to be evaluated at the point under study.

Characteristic Equations

To examine the stability of the motion of the infinitesimal body near any of the equilibrium points, we take their trial solutions as

$$\xi = Ae^{\lambda t},$$
$$\eta = Be^{\lambda t}. \qquad (15)$$

Differentiating Eq. (15) with respect to t, we have

$$\dot{\xi} = A\lambda e^{\lambda t}, \dot{\eta} = B\lambda e^{\lambda t}$$
$$\ddot{\xi} = A\lambda^2 e^{\lambda t}, \ddot{\eta} = B\lambda^2 e^{\lambda t}. \qquad (16)$$

Putting Eqn.(16) into Eqn.(14), we get

$$A\lambda^2 e^{\lambda t} - 2nB\lambda e^{\lambda t} = A\Omega^0_{xx}e^{\lambda t} + B\Omega^0_{xy}e^{\lambda t},$$
$$B\lambda^2 e^{\lambda t} + 2nA\lambda e^{\lambda t} = A\Omega^0_{xy}e^{\lambda t} + B\Omega^0_{yy}e^{\lambda t}.$$

Collecting like terms, the last two equations become

$$A\left(\lambda^2 - \Omega^0_{xx}\right)e^{\lambda t} - B\left(\Omega^0_{xy} + 2n\lambda\right)e^{\lambda t} = 0,$$
$$-A\left(\Omega^0_{xy} - 2n\lambda\right)e^{\lambda t} + B\left(\lambda^2 - \Omega^0_{yy}\right)e^{\lambda t} = 0. \qquad (17)$$

System (17), has solutions if

$$\begin{vmatrix} \lambda^2 - \Omega^0_{xx} & -\Omega^0_{xy} - 2n\lambda \\ 2n\lambda - \Omega^0_{xy} & \lambda^2 - \Omega^0_{yy} \end{vmatrix} = 0. \qquad (18)$$

Equation (18) can be written as

$$\left(\lambda^2 - \Omega^0_{xx}\right)\left(\lambda^2 - \Omega^0_{yy}\right) + \left(2n\lambda + \Omega^0_{xy}\right)\left(2n\lambda - \Omega^0_{xy}\right) = 0$$

or

$$\lambda^4 + \left(4n^2 - \Omega^0_{yy} - \Omega^0_{xx}\right)\lambda^2 + \Omega^0_{xx}\Omega^0_{yy} - \left(\Omega^0_{xy}\right)^2 = 0 \qquad (19)$$

Equation (19) is called the characteristic equation corresponding to the variational equation of Eq. (13).

Stability Analysis of the collinear equilibrium points

This section examines the collinear equilibrium points obtained for the EQ Pegasi system in terms of stability. So, using Eqns. (9a), (9b) and (9b) the following systems are obtained:

$$\Omega_{xx} = n^2 - \frac{(1-\mu)}{r_1^3}\left(1 + \frac{3A_1^*}{2r_1^2} - \frac{15A_2^*}{8r_1^4} + \frac{35A_3^*}{16r_1^6}\right) + \frac{3(1-\mu)(x-\mu)^2}{r_1^5}\left(1 + \frac{5A_1^*}{2r_1^2} - \frac{35A_2^*}{8r_1^4} + \frac{105A_3^*}{16r_1^6}\right)$$
$$- \frac{\mu}{r_2^3}\left(1 + \frac{3A_1^{**}}{2r_2^2} - \frac{15A_2^{**}}{8r_2^4} + \frac{35A_3^{**}}{16r_2^6}\right) + \frac{3\mu(x+1-\mu)^2}{r_2^5}\left(1 + \frac{5A_1^{**}}{2r_2^2} - \frac{35A_2^{**}}{8r_2^4} + \frac{105A_3^{**}}{16r_2^6}\right),$$

$$\Omega_{xy} = 0,$$

$$\Omega_{yy} = n^2 - \frac{(1-\mu)}{r_1^3}\left(1 + \frac{3A_1^*}{2r_1^2} - \frac{15A_2^*}{8r_1^4} + \frac{35A_3^*}{16r_1^6}\right) + \frac{3(1-\mu)y^2}{r_1^5}\left(1 + \frac{5A_1^*}{2r_1^2} - \frac{35A_2^*}{8r_1^4} + \frac{105A_3^*}{16r_1^6}\right)$$
$$- \frac{\mu}{r_2^3}\left(1 + \frac{3A_1^{**}}{2r_2^2} - \frac{15A_2^{**}}{8r_2^4} + \frac{35A_3^{**}}{16r_2^6}\right) + \frac{3\mu y^2}{r_2^5}\left(1 + \frac{5A_1^{**}}{2r_2^2} - \frac{35A_2^{**}}{8r_2^4} + \frac{105A_3^{**}}{16r_2^6}\right), \qquad (20)$$

Next, with $y = 0$, the value of each collinear equilibrium point, x_0 as well as the mean motion n^2 in Eqn. (8) is substituted into Eqns. (20) to get:

$$\Omega_{xx}^{0}=\left\{1+\frac{3}{2}\left(A_1^{*}+A_1^{**}\right)-\frac{15}{8}\left(A_2^{*}+A_2^{**}\right)+\frac{35}{16}\left(A_3^{*}+A_3^{**}\right)\right\}+\frac{2(1-\mu)}{r_1^{3}}\left(1+\frac{3A_1^{*}}{r_1^{2}}-\frac{45A_2^{*}}{8r_1^{4}}+\frac{35A_3^{*}}{4r_1^{6}}\right)$$
$$+\frac{2\mu}{r_2^{3}}\left(1+\frac{3A_1^{**}}{r_2^{2}}-\frac{45A_2^{**}}{8r_2^{4}}+\frac{35A_3^{**}}{4r_2^{6}}\right), \quad (21)$$

and

$$\Omega_{yy}^{0}=\left\{1+\frac{3}{2}\left(A_1^{*}+A_1^{**}\right)-\frac{15}{8}\left(A_2^{*}+A_2^{**}\right)+\frac{35}{16}\left(A_3^{*}+A_3^{**}\right)\right\}-\frac{(1-\mu)}{r_1^{3}}\left(1+\frac{3A_1^{*}}{2r_1^{2}}-\frac{15A_2^{*}}{8r_1^{4}}+\frac{35A_3^{*}}{16r_1^{6}}\right)$$
$$-\frac{\mu}{r_2^{3}}\left(1+\frac{3A_1^{**}}{2r_2^{2}}-\frac{15A_2^{**}}{8r_2^{4}}+\frac{35A_3^{**}}{16r_2^{6}}\right),$$

with (22)

$$r_1^{2}=\left(x_0-\mu\right)^{2}\Rightarrow r_1=\left|x_0-\mu\right|,$$
$$r_2^{2}=\left(x_0+1-\mu\right)^{2}\Rightarrow r_2=\left|x_0+1-\mu\right|.$$

We present the results in Table 8 by substituting the following equations (21) and (22) in eqn. (19) and solving for the equation's roots at each collinear equilibrium point.

Table 7: Roots of the characteristic equation in the system (18) at $L_{1,2,3}$ using the required data from Tables 3 and 4

Case	$\lambda_{1,2,3,4}^{L_1}$	$\lambda_{1,2,3,4}^{L_2}$	$\lambda_{1,2,3,4}^{L_3}$
1	±3.90536224 ± 2.88211907*i*	±0.93348912 ±1.21871929*i*	±1.42046984 ±1.44918227*i*
2	±3.96481749 ±2.89410319*i*	±0.93817275 ±1.21933750*i*	±1.43081285 ±1.44831372*i*
3	±4.02247645 ±2.90610093*i*	±0.94285784 ±1.21995835*i*	±1.44102601 ±1.44752190*i*
4	±4.07851961 ±2.91810475*i*	±0.94754462 ±1.22058205*i*	±1.45111377 ±1.44680312*i*
5	±4.13309982 ±2.93010814*i*	±0.95223331 ±1.22120881*i*	±1.46108012 ±1.44615383*i*
6	±4.18634929 ±2.94210626*i*	±0.95692228 ±1.22183808*i*	±1.47093087 ±1.44557164*i*
7	±4.23838223 ±2.95409511*i*	±0.96161304 ±1.22247059*i*	±1.48066843 ±1.44505289*i*
8	±4.28929763 ±2.96607124*i*	±0.96630393 ±1.22310577*i*	±1.49029711 ±1.44459504*i*
9	±4.33918296 ±2.97803211*i*	±0.97099651 ±1.22374434*i*	±1.49982089 ±1.44419568*i*

RESULTS AND DISCUSSION

The location and stability of CEPs of any of the five Nigerian Satellites in the R3BP for the oblate EQ Pegasi system are being studied. The zonal harmonic effects of EQ Pegasi A and EQ Pegasi B have been taken into consideration. More particularly, the works of Abouelmagd *et al.*, (2012; 2015a) have been extended to include the J_6 zonal harmonics terms for both primaries. In Tables 4, 5, and 6, it can be seen that the positions of the CEPs, $L_{1,2,3}$ shift slightly as the

zonal harmonics up to J_6 (A_3^*, and A_3^{**}) are varied across the cases (1 through 9) (that is L_1 and L_2 move closer to the origin while L_3 moves away from the origin). For example, in Case 1 of Table 4, the positions of $L_{1,2,3}$ are -0.2470833, 1.1339893, and -1.2505497, respectively with corresponding Jacobian constants, $C_{L_{1,2,3}}$ as 3.9666881**,** 3.3313783**,** and 3.5658325**.** These values change slightly as the parameters vary across the nine cases, showing the influence of J_6. Similarly, the same can be observed for J_4 (A_2^*, A_2^{**}) and J_2 (A_1^* and A_1^{**}) in Tables 5 and 6, respectively. The zonal harmonic J_2 (A_1^* and A_1^{**}) (equatorial bulge) has the most significant impact on the positions of the CEPs as shown in Table 6. Figure 5illustrates the behavior of the CEPs under various trends. In the case of L_1, the gray lines indicate a slight rightward shift toward the secondary mass, suggesting that the equatorial bulge increases the secondary's gravitational attraction compared to that of the primary. The magenta and blue lines, which represent J_4 and further adjust this effect to reflect asymmetries of higher order in mass distribution. In the case of L_2, the gray lines illustrate a leftward movement toward the origin instigated by J_2, which signifies a compression of the potential well resulting from oblateness. The magenta and blue lines imply that J_4 and J_6 may either strengthen or counter this shift based on their particular contributions. For L_3, the gray lines illustrate a movement to the left that is separate from the origin, suggesting that the primary's effective gravitational influence has broadened. The higher-order terms, depicted by magenta and blue lines, can either amplify this trend or bring about oscillatory behaviour. In sum, Figure 5 illustrates the progressive refinement of the gravitational potential by each zonal harmonic, with J_4 and J_6 introducing subtle perturbations that displace the CEPs beyond the primary influence of J_2.

The Jacobian constants, representing the energy levels at the equilibrium points, vary across the cases, as shown in Tables 4, 5, and 6. The inclusion of J_2, J_4, and J_6 modifies the gravitational potential, leading to changes in the energy required for a satellite to remain near these points. However, the changes in the Jacobian constants are relatively small, indicating that the lower-order term still dominates the overall dynamics J_2.

Equation (18), the characteristic equation derived from the variational equations in Equation (13), assesses the stability of equilibrium points by analyzing the nature of its roots (real, imaginary, or complex). The Lyapunov theorem, applied via the indirect method, indicates that stability depends on the roots of the characteristic equation. Negative real parts signify asymptotic stability, positive real parts indicate instability, and purely imaginary roots render the analysis inconclusive. Consequently, the nature of the roots is directly connected to the stability outcomes.

The roots of the characteristic equation of eqn. 18 are presented in Table 7 for cases 1 through 9. These are complex roots with positive real parts, confirming that the CEPs are unstable, even when accounting for the effects of the zonal harmonics J_2, J_4, and J_6. The instability of the CEPs implies that a satellite placed near these points will not remain there indefinitely without active station-keeping. This is particularly relevant for mission design and trajectory optimization. Also, this result is consistent with the classical R3BP, where collinear points are known to be unstable.

The inclusion of J_2, J_4, and J_6 modifies the positions of the CEPs and their stability characteristics, but the fundamental instability of the CEPs remains, and these results are in conformity with (Reigber, 1989). These results are also in agreement with those of Abouelmagd (2012) when only the zonal harmonic terms J_2 and J_4 of the bigger primary studies is considered Abouelmagd *et al.*, (2015a), when the J_2 and J_4 zonal harmonic terms of both primaries are taken into cognizance.

The zonal harmonics terms J_4 and J_6 account for higher-order deformations in the gravitational potential, introducing additional complexities into the system's dynamics. While these terms have a noticeable impact on the positions of the equilibrium points and their Jacobian constants, it is seen that their effect is relatively small compared to J_2. These findings underscore the importance of accounting for higher-order gravitational effects in the design and stability analysis of precise missions, particularly for Nigerian satellites operating in complex gravitational environments.

CONCLUSION

In conclusion, a rebalancing of gravitational forces is suggested by the slight changes in CEP locations (e.g., L_1 and L_2 coming closer to the origin, L_3 moving outward) with increasing zonal harmonics. The colour-

coded patterns in Figure 5 show that J_4 and J_6 introduce slight asymmetries, whereas J_2's prominence emphasizes the equatorial bulge's role in flattening the potential well. Moderate changes in the Jacobian constants (from 3.9666881 to 3.5658325 in Case 1) show that energy levels react to oblateness but are mostly affected by lower-order terms.

For Nigerian satellites, this instability underscores the need for effective station-keeping measures, particularly in binary systems like EQ Pegasi, where tidal and rotational forces heighten disturbances. These insights refine mission planning by detailing how higher-order gravitational terms impact orbit design, a key factor given Nigeria's equatorial launch benefits.

The research assumes constant oblateness parameters, overlooking changes from stellar evolution or mass transfer in EQ Pegasi. It also treats the satellite as a point mass, disregarding its shape or orientation effects.Validation is constrained by the absence of real-time observational data for EQ Pegasi, and computational limits cap the analysis at J_6, excluding higher harmonics like J_8.

The future scope of this study may include taking into cognizance all or part of the following:

- Expand the framework to incorporate higher-order zonal harmonics (beyond J_6) for a more accurate gravitational field representation; possibly use machine learning techniques to manage the computational complexity.
- Examine the effects of mass transfer between the white dwarf and red dwarf stellar components of EQ Pegasi on equilibrium point evolution and long-term stability.
- Work with NASRDA to incorporate real-time data from Nigerian satellites to empirically validate the model in real binary system conditions.
- Analyze how spacecraft geometry and attitude dynamics impact orbital behavior, going beyond the point-mass approximation to improve practical applicability.

To support Nigeria's ambitious 2030 lunar exploration goals, the improved methodology should be applied to other prominent binary systems (such as Sirius and Procyon) to establish broader astrophysical insights.

Acknowledgments

This work was made possible by the Nigeria Tertiary Education Trust Fund (TETFUND) research grant for 2024, for which the first author is truly grateful.

REFERENCE

Abdouelmagd, E. I. (2012). Existence and stability of triangular points in the restricted three-body problem with numerical applications. *Astrophysics and space science*, 342, 45-53. Doi: 10.1007/s10509-012-1162-y

Abouelmagd, E.I., Alhothuali, M.S., Guirao, J.L.G., & Malaikah, H.M. (2015a). The effect of zonal harmonic coefficients in the framework of the restricted three-body problem. *Advances in Space Research*, 55:1660–1672. http://dx.doi.org/10.1016/j.asr.2014.12.030

Abouelmagd, E.I., Alhothuali, M.S., Guirao, J.L.G,& Malaikah, H.M. (2015b). Periodic and secular solutions in the restricted three-body problem under the effect of zonal harmonic Parameters. *Appl. Math. Inf. Sci.***9**(4), 1659.

Arredondo, J.A., Guo, J., Stoica, C., & Tamayo, C. (2012). On the restricted three body problem with oblate primaries. *Astrophys. Space Sci.***341**(2), 315. https://doi.org/10.1007/s10509-012-1085-7

Baresi, N. & Dell'Elce, L. (2023). Periodic and Quasi-Periodic Orbits near Close Planetary Moons. *Journal of Guidance, Control, and Dynamics* , 46(6445):1-15.DOI:10.2514/1.G007221

Bury, L., & McMahon, J. (2020). The effect of zonal harmonics on dynamical structures in the circular restricted three-body problem near the secondary body. *Celestial Mechanics and Dynamical Astronomy, 132:45.* https://doi.org/10.1007/s10569-020-09983-3

Crosley, M. K. & Osten, R. A. (2018). Constraining Stellar Coronal Mass Ejections through Multi-wavelength Analysis of the Active M Dwarf EQ Peg. *The Astrophysical Journal*. **856** (1). 39. doi:10.3847/1538-4357/aaaec

Fabian, A. C., Sanders, J. S., Allen, S. W., & Crawford, C. S. (2012). The mass profile of the coma cluster of galaxies. *Monthly Notices of the Royal Astronomical Society*, 421(1), 25-34.

Gyegwe, J. M., Vincent, A. E. & Perdiou, A. E. (2022). On the stability of the equilibrium points in the photogravitational R3BP with an oblate infinitesimal and triaxial primaries for the binary Lalande 21258 system. Daras, N.J, Rassias T.M. (eds.), *Approximation and Computation in Science and Engineering*, Springer Optimization and Its Application, 180, 397-415. https://doi.org/10.1007/978-3-030-84122-5_21

Jagadish, S., Kalantonis,V. S., Gyegwe, J. M**.** & Perdiou, A. E. (2016). Periodic motions around the collinear equilibrium points of the restricted three-body problem where the primary is a triaxial rigid body and

secondary is an oblate spheroid. *The Astrophysical Journal Supplement series, 277*, 13. DOI:10.3847/0067-0049/227/2/13

Jain, M. & Aggarwal, R. (2015). Restricted three-body problem with Stokes Drag effect. *International Journal of Astronomy and Astrophysics*, **5**, 95-105. doi: 10.4236/ijaa.2015.52013.

Johnston. R. (2022). List of nearby stars to 26 light years. https://www.johnstonsarchive.net/astro/nearstar.html. Retrieve on the 11th of April, 2024.

Kalantonis, V. S. (2025). Exploring the Influence of Oblateness on Asymptotic Orbits in the Hill Three-Body Problem. *AppliedMath*, *5*(1). https://doi.org/10.3390/appliedmath5010030

Kalantonis, V. S., Vincent, A. E., Gyegwe**,** J.M.& Perdios, E. A. (2021). Periodic solutions around the out-of-plane equilibrium points in the restricted three-body problem with radiation and angular velocity variation. *Nonlinear Analysis and Global Optimization, Springer Optimization and Its Applications*, 167. https://doi.org/10.1007/978-3-030-61732-5_11

Katour, D.A., Abd El-Salam, F.A. & Shaker, M.O. (2014). Relativistic restricted three body problem with oblatness and photo-gravitational corrections to triangular equilibrium points. *Astrophys Space Sci* , **351**, 143–149 (2014). https://doi.org/10.1007/s10509-014-1826-x

Lambeck, K. (1988). Geophysical geodesy: The slow deformations of the Earth. Clarendon Press.

Murray, C. D., & Dermott, S. F. (1999). Solar system dynamics. Cambridge University Press.

Oni, L., Cyril-Okeme, V., Stephen, S. & Gyegwe, J. M. (2024). Investigating Motion around out-of-plane points in the restricted three-body problem with variable shape and masses. *New Astronomy*, 114 (2025) 102311. https://doi.org/10.1016/j.newast.2024.102311

Oyewole, S. (2017). Space Research and Development in Africa. *Astropolitics*, 15(2), 185- 208. DOI: 10.1080/14777622.2017.1339254

Oyewole, S. (2024). Utilitarianism in Outer Space: Space Policy Socioeconomic Development and Security Strategies in Nigeria and South Africa. Springer Cham, https://doi.org/10.1007/978-3-031-49646-2

Pan, S. & Hou, X . (2022). Analysis of Resonance Transition Periodic Orbits in the Circular Restricted Three-Body Problem. Appl. Sci. 2022, 12, 8952. https://doi.org/10.3390/app12188952

Putra, L.B., Huda, I.N., Ramadhan, H.S., Saputra, M.B. & Hidayat, T. (2024). Effects of variable mass, disk-like structure, and radiation pressure on the dynamics of circular restricted three-body problem. Romanian Astronomical Journal, 34(1-2), 33-47. DOI 10.59277/RoAJ.2023.1-2.03

Reigber, C. (1989). Gravity field and steady-state ocean circulation from satellite altimetry. *Journal of Geophysical Research: Solid Earth*, 94(B9), 11821-11833.

Roy, A.E. (2005). Orbital Motion, 4th edn. Institute of Physics Publishing, Bristol.

Singh, J & Richard, T.K. (2022). A study on the positions and velocity sensitivities in the restricted three-body problem with radiating and oblate primaries, *New Astronomy* 2021, 101704. DOI:10.1016/j.newast.2021.101704

Singh, J. & Ashagwu, B.S. (2024). Combined effect of Poynting-Robertson (P-R) drag, oblateness and radiation on the triangular points in the elliptic restricted three-body problem. Scientific reports, 14, 11564. https://doi.org/10.1038/s41598-024-61935-1

Singh, J., Kalantonis, V.S., Gyegwe, J. M. & Perdiou, A. E. (2016). Periodic motions around the collinear equilibrium points of the restricted three-body problem where the primary is a triaxial rigid body and secondary is an oblate spheroid. *The Astrophysical Journal Supplement series, 277*, 13. DOI:10.3847/0067-0049/227/2/13

Singh, J., Perdiou, A. E., Gyegwe, J. M. & Kalantonis, V. S. (2017). Periodic orbits around the collinear equilibrium points for binary Sirius, Procyon, Luhman 16, α-Centuari and Luyten 726-8 systems: the spatial case. *Journal of physics communications*, 1 (2017) 025008. https://doi.org/10.1088/2399-6528/aa8976

Singh, J., Perdiou, A. E., Gyegwe, J. M. & Perdios, E.A. (2018). Periodic solutions around the collinear equilibrium points in the perturbed restricted three-body problem with triaxial and radiating primaries for the binary HD 191408, Kruger 60 and HD 155876 systems. *Applied Mathematics and Computation*, 325 (2018) 358-374. https://doi.org/10.1016/j.amc.2017.11.052

Szebehely, V. (1967). Theory of Orbits—The Restricted Problem of Three Bodies. Academic Press, New York.